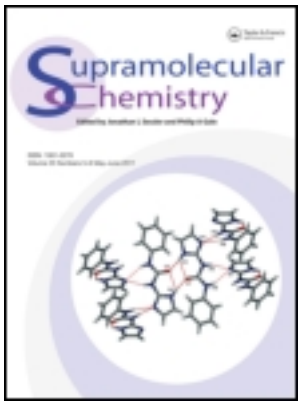

Supramolecular Chemistry
Publication details, including instructions for authors and subscription information:
http://www.tandfonline.com/loi/gsch20

Molecular capsules and coordination polymers from a backbone-modified cyclic peptide bearing pyridyl arms

Ying Dong [a], David T.J. Loong [a], Alex K.L. Yuen [a], Richard J. Black [a], Shane O'Malley [a], Jack K. Clegg [a], Leonard F. Lindoy [a] & Katrina A. Jolliffe [a]
[a] School of Chemistry, The University of Sydney, 2006 NSW, Australia
Version of record first published: 20 Jun 2012.

To cite this article: Ying Dong, David T.J. Loong, Alex K.L. Yuen, Richard J. Black, Shane O'Malley, Jack K. Clegg, Leonard F. Lindoy & Katrina A. Jolliffe (2012): Molecular capsules and coordination polymers from a backbone-modified cyclic peptide bearing pyridyl arms, Supramolecular Chemistry, 24:7, 508-519

To link to this article: http://dx.doi.org/10.1080/10610278.2012.688128

Supramolecular Chemistry
Vol. 24, No. 7, July 2012, 508–519

Taylor & Francis
Taylor & Francis Group

Molecular capsules and coordination polymers from a backbone-modified cyclic peptide bearing pyridyl arms

Ying Dong, David T.J. Loong, Alex K.L. Yuen, Richard J. Black, Shane O'Malley, Jack K. Clegg, Leonard F. Lindoy and Katrina A. Jolliffe*

School of Chemistry, The University of Sydney, 2006 NSW, Australia

(*Received 13 March 2012; final version received 18 April 2012*)

A tris-pyridyl-substituted *Lissoclinum*-type cyclic peptide forms a trinuclear molecular capsule on addition of Ag(I) ions and an infinite one-dimensional coordination polymer on addition of Pd(II) ions.

Keywords: cyclic peptide; metallo-supramolecular chemistry

Introduction

Metal-directed self-assembly has been widely used to construct both discrete architectures such as helicates, capsules and cages (*1–4*) and larger aggregates such as coordination polymers (*5*). The metal ion-directed self-assembly of discrete systems incorporating a central cavity is of particular interest. One of the major challenges in this area is the design of scaffolds bearing multiple ligands, which can be directed, upon addition of an appropriate metal ion, to form pre-determined architectures. One class of molecular scaffold, which has been little explored in this area, is backbone-modified cyclic peptides.

Analogues of the *Lissoclinum* class of cyclic peptides (*6*) have found application as receptors for anions (*7, 8*), cations (*9*) and neutral molecules (*10*); as scaffolds for the display of peptide architectures (*11*); as stabilisers of G-quadruplex structure (*12*); as chiral tripodal ligands for metal ions (*13*) and in the preparation of covalent cage structures (*8, 14*). However, to date, the ability of these scaffolds to form well-defined metallo-supramolecular architectures by self-assembly has not been examined. The structure of this class of backbone-modified cyclic peptide, resulting from a network of bifurcated hydrogen bonds between the amide protons and azole nitrogen atoms in the macrocycle, lends itself to the display of multiple ligands for metal binding with well-defined geometry. If all amino acids are of the same configuration, the side chains project from one face of the peptide scaffold, in an arrangement similar to that observed for other macrocyclic scaffolds such as the resorcinarenes (*2, 3*) and cyclotriveratrylene (*4*). Functionalisation of these side chains with ligands should allow, upon addition of metal ions with the appropriate coordination geometry, the formation of self-assembled molecular capsules or coordination polymers in a manner similar to that observed for the macrocyclic scaffolds described above. We report here our initial studies involving the functionalisation of a *Lissoclinum*-type cyclic peptide with pyridyl ligands to provide **1** and the interactions of this molecule with silver(I) and palladium(II) ions to form a molecular capsule and coordination polymer, respectively.

Results and discussion

Both the metal ion properties (charge, radius, spin state, preferred coordination geometry and kinetic inertness) and those of the organic components (shape, flexibility and electronics) play important roles in the self-assembly process. We designed our cyclic peptide scaffold such that a variety of ligands could readily be appended to enable future exploration of the effect of ligand structure on self-assembly processes. This led to the design of scaffold **2** in which ethylenebromide side chains are appended to the scaffold. We envisaged that these side chains would be flexible enough to allow the formation of both molecular capsules and coordination polymers depending on the coordination geometry required by the added metal ions, while being short enough to prevent the formation of simple complexes in which one metal ion is bound to a single cyclic peptide through all three ligands. As proof of principle, we chose to use pyridyl groups to functionalise the scaffold as these have previously been widely utilised as ligands in the formation of self-assembled metallo-supramolecular structures (*15, 16*).

There are a number of approaches to the synthesis of trimeric scaffolds such as **2** (*17, 18*), the most attractive of which involves the cyclooligomerisation of an appropriately side-chain-protected oxazole (*17*). Therefore, our

*Corresponding author. Email: kate.jolliffe@sydney.edu.au

ISSN 1061-0278 print/ISSN 1029-0478 online

http://dx.doi.org/10.1080/10610278.2012.688128
http://www.tandfonline.com

initial synthetic target was the homoserine-derived oxazole building block **3**. We first coupled Boc-Hse(Bn)-OH with threonine methyl ester using diphenylphosphoryl azide (DPPA) as the coupling reagent to give the dipeptide **4** in 62% yield (Scheme 1). Treatment of **4** with deoxofluor, followed by immediate oxidation of the intermediate oxazoline with 1,8-diazabicycloundec-7-ene (DBU) and $BrCCl_3$ (*19*), gave the oxazole **3** in 50% yield. Single crystals of **3** were grown by the slow evaporation of an acetone solution (see Supplementary Information available online for details).

It has previously been established that the choice of peptide-coupling agent for the cyclooligomerisation of azole heterocycle-derived amino acids can significantly affect both the cyclisation yield and ratio of cyclotrimer to cyclotetramer (*18*). Therefore, we examined the cyclooligomerisation reaction under two sets of conditions. Hydrolysis of the methyl ester of **3** upon treatment with aqueous sodium hydroxide gave carboxylic acid **5** which was either subjected to Boc-deprotection upon treatment with HCl in dioxane to give amino acid **6** or subjected to reaction with pentafluorophenol in the presence of dicyclohexylcarbodiimide (DCC) to give the activated ester **7** which was subsequently Boc-deprotected upon treatment with trifluoroacetic acid to give the amino salt **8**. Treatment of **6** with pentafluorophenyldiphenylphosphinate (FDPP) resulted in cyclooligomerisation to provide the cyclic trimer **9** in 42% yield (Scheme 2). While traces of the cyclic tetramer **10** were observed by mass spectrometry of the crude reaction mixture, this was not isolated. In contrast, treatment of the preformed pentafluorophenyl ester **8** with diisopropylethylamine gave both the cyclic trimer **9** (52%) and cyclic tetramer **10** (18%) as isolable compounds.

To install the bromide functional groups on the cyclic peptide scaffold, the side-chain benzyl-protecting groups were removed upon hydrogenolysis of **9** to give the triol **11** (Scheme 3). A number of attempts were made to directly convert the triol **11** into tribromide **2**; however, these

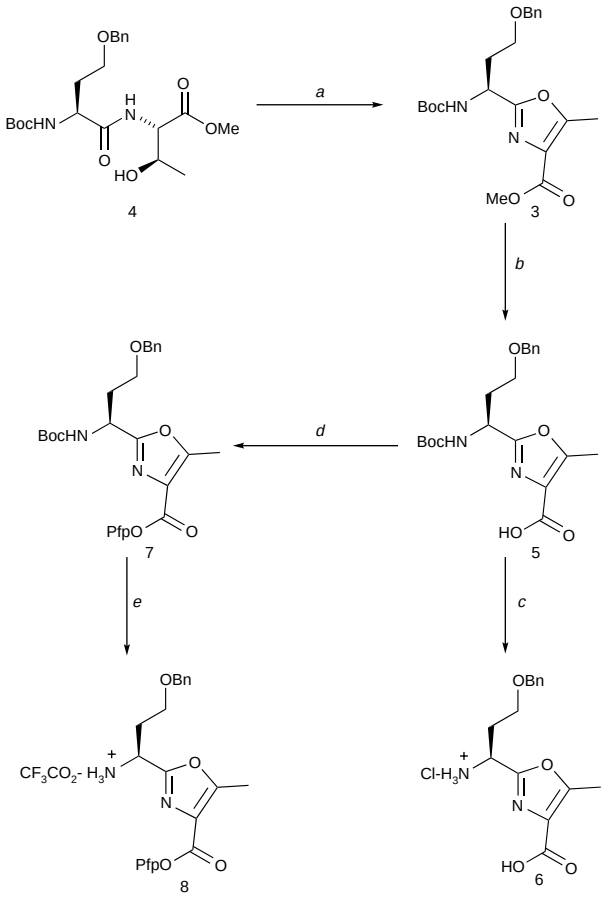

Scheme 1. Synthesis of oxazole building blocks. Conditions: (*a*) *i)* deoxofluor, CH_2Cl_2, −20°C – rt; *ii)* DBU, $BrCCl_3$, CH_2Cl_2, 50% over two steps; (*b*) NaOH, MeOH, H_2O, quant.; (*c*) 4 M HCl in dioxane, 96%; (*d*) pentafluorophenol, DCC, THF, 81%; (*e*) CF_3CO_2H, CH_2Cl_2, quant.

were all low yielding or gave mixtures that were difficult to purify. Therefore, **11** was firstly treated with *p*-toluenesulfonylchloride to give the tritosylate **12** in 95% yield, then subsequent substitution of the tosylate groups with LiBr gave the tribromide **2** in 85% yield. Treatment of

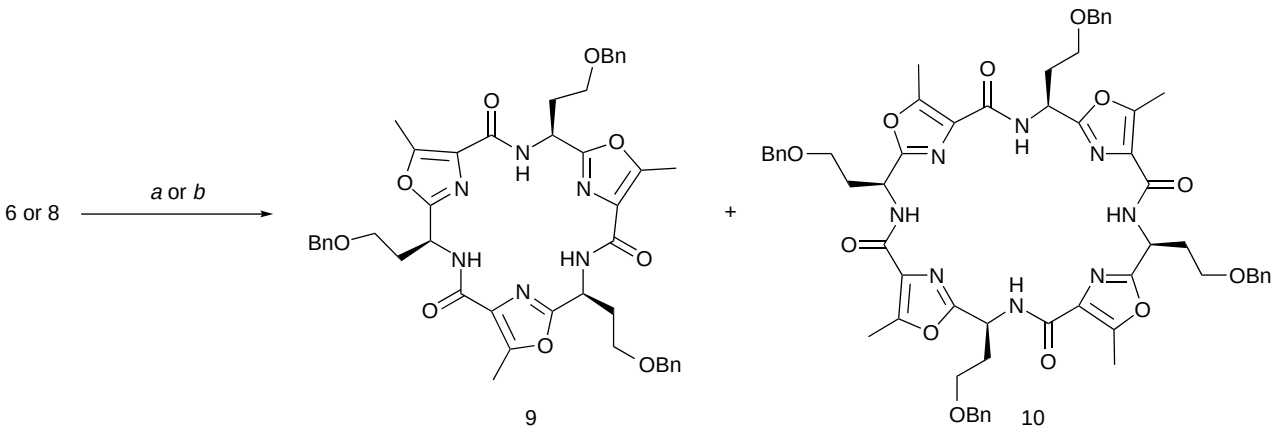

Scheme 2. Conditions: (*a*) **6**, FDPP, $^{i}Pr_2NEt$, DMF, 0.05 M; (*b*) **8**, $^{i}Pr_2NEt$, DMF, 0.05 M.

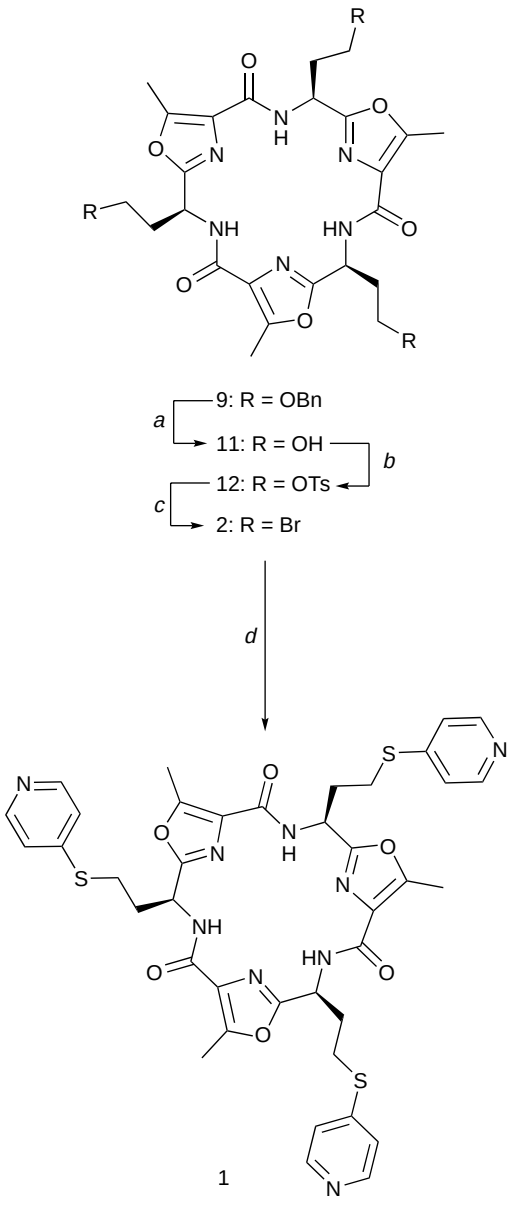

Scheme 3. Conditions: (*a*) H_2, Pd/C, CH_3OH, ethyl acetate, 99%; (*b*) *p*-toluenesulphoonylchloride, Et_3N, Me_3N.HCl, CH_3CN, 95%; (*c*) LiBr, DMF, 55°C, 85%; (*d*) 4-mercaptopyridine, Cs_2CO_3, CH_3CN, 84%.

2 with 4-mercaptopyridine in the presence of caesium carbonate gave the required pyridyl-functionalised scaffold **1** in 84% yield.

Crystals of the intermediate tribromide **2**·0.25CH_2Cl_2·0.875MeOH·0.625H_2O suitable for diffraction studies were grown from the slow evaporation of a dichloromethane/methanol solution (Figure 1). Tribromide **2** crystallises in the monoclinic space group $P2_1$ with two cyclic peptides in the asymmetric unit. The refined Flack parameter (*20*) (0.075(14)) confirms the enantiopurity of the structure. In a similar manner to the crystal structures of the oxazole-containing cyclic peptides and cryptands

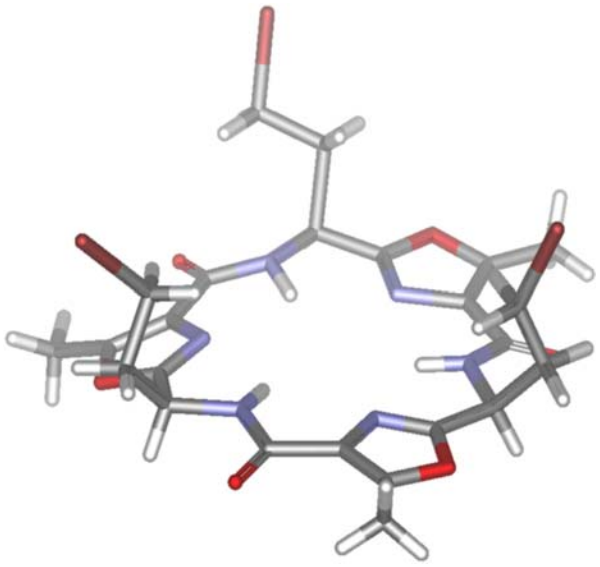

Figure 1. Structure of one of the two macrocycles in crystal structure of **2**. Disorder and solvent removed for clarity.

(*8*) that we have previously reported, the macrocycle is largely planar with one of the oxazole rings tilted slightly out of the plane; an arrangement stabilised by intramolecular hydrogen bonding.

Each of the disordered bromoethyl side chains projects from the same face of the macrocycle, and adjacent macrocycles pack closely together in a dimeric arrangement such that the side chain of one peptide is directed towards the centre of the adjacent peptide taking advantage of weak hydrogen bonding interactions (NH···Br = 2.35–2.94 Å; Figure 2). These dimers further interact with adjacent pairs of molecules through weak offset face-to-face oxazole–oxazole π-stacking indicated by a ring centroid–centroid separation of 3.5 Å, resulting in the formation of infinite undulating 1D polymers extending along the crystallographic *b*-axis.

With the tri(pyridyl) functionalised scaffold **1** in hand, we chose to examine the formation of complexes with both silver(I) and palladium(II) as both of these have frequently been used in the formation of self-assembled metallo-supramolecular structures using pyridyl ligands and provide access to different coordination geometries (*3*, *4*, *15*, *16*).

Addition of a solution of silver nitrate in methanol/acetonitrile (1:1) to a solution of **1** in methanol resulted in immediate precipitation of a colourless solid, the microanalysis of which confirmed a stoichiometry of $L_2Ag_3(NO_3)_3$ (L = **1**). The positive ion mass spectrum [electrospray ionisation (ESI)] of this complex revealed a peak corresponding to $[L_2Ag_3(NO_3)_2]^+$ (m/z = 2099 for the parent ion) with an isotopic distribution pattern which matched that calculated for this ion (Figure 3). Similarly,

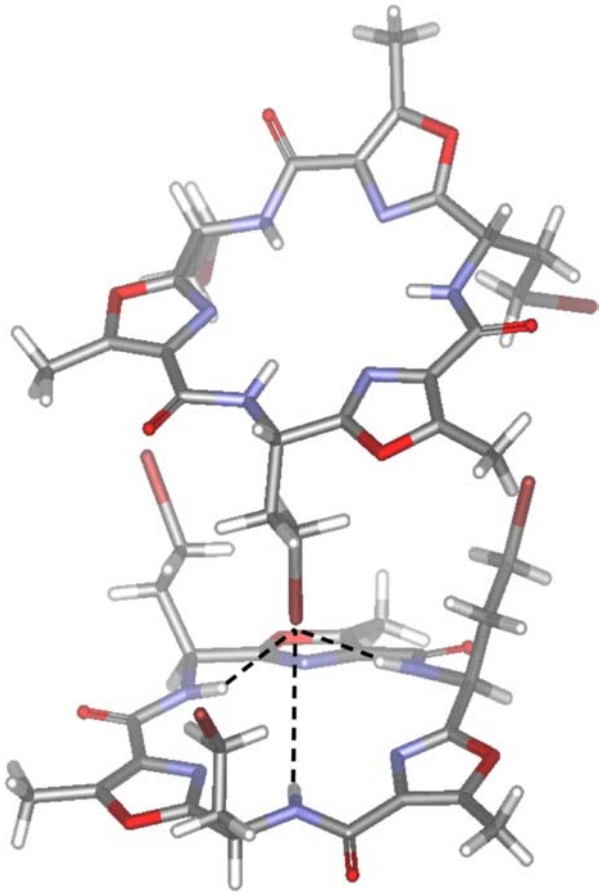

Figure 2. Dimeric arrangement observed in crystal structure of **2**. Dashed lines indicate intermolecular hydrogen bonds.

the mass spectrum of a sample of **1** after addition of silver hexafluorophosphate gave a parent peak at $m/z = 2265$ and an isotopic distribution pattern corresponding to the desired silver(I) cage stoichiometry of $L_2Ag_3(PF_6)_2^+$. The ^{1}H nuclear magnetic resonance (NMR) spectra of mixtures of **1** and silver hexafluorophosphate in deuteromethanol, deuterodimethylsulphoxide or deuteroacetonitrile resulted in small downfield shifts (<0.2 ppm) of the signals attributable to the pyridyl protons. The signals remained sharp, indicating that the C_3 symmetry of **1** was maintained and that the silver sites were equivalent in all three solvents. Unfortunately, single crystals of this complex could not be obtained. The structure of $[L_2Ag_3]^{3+}$ was modelled using the semi-empirical AM1 level in Spartan 10 (Figure 4). The modelled structure shows the expected coordination between the silver ions and the pyridyl nitrogen rings, in analogy to the simpler benzene-derived metallo-capsule previously reported by Bray et al. (*16*). Notably, in this case, the chiral nature of the cyclic peptide scaffold is reflected in a slight helical twist of the self-assembled structure.

In contrast to the behaviour observed with silver(I) ions, addition of Pd(dppp)OTf_2 to a solution of cyclic peptide **1** in methanol resulted in immediate precipitation of a colourless solid. This was redissolved in $CDCl_3$, and significant broadening of all signals in the ^{1}H NMR spectrum and a loss of the C_3 symmetry of **1** were observed. No change in the spectrum was observed after standing at room temperature (rt) for 7 days. Slow diffusion of diethyl ether into this mixture yielded a small number of colourless plate-like crystals suitable for X-ray studies, which revealed a polymeric complex of composition $\{[Pd(dppp)\mathbf{1}]\cdot OTf\cdot Cl\cdot 3MeOH\cdot 3Et_2O\}_n$ had formed (Figure 5). The Pd(dppp)OTf_2 was obtained from reaction of Pd(dppp)Cl_2 with excess silver triflate (*21*). Presumably, the chloride ions in $\{[Pd(dppp)\mathbf{1}]\cdot OTf\cdot Cl\cdot 3MeOH\cdot 3Et_2O\}_n$ are present as a result of a small amount of chloride remaining in the Pd(dppp)OTf_2 sample due to incomplete ligand exchange. The complex crystallises in the enantiomorphic chiral space group $P3_121$, and the refined Flack (*20*) parameter (0.02(5)) confirms the enantiopurity of the peptide. The *cis*-Pd(II) centres are square planar, coordinated to the bidentate dppp ligand and pyridyl ligands from two different cyclic peptides forming a coordination polymer that extends along the crystallographic *a*-axis. One of the pyridyl groups from the peptide remains uncoordinated, reflecting the loss of C_3 symmetry observed in solution. Each of the coordinated pyridines undergoes offset face-to-face $\pi-\pi$ interactions with the adjacent phenyl rings of the dppp ligands (centroid–centroid distances of 3.63 and 3.65 Å).

The macrocyclic units are once again largely planar, stabilised by intramolecular hydrogen bonding. The triflate counterions are just above the face of the cyclic peptide with one of the oxygen atoms hydrogen bonded by the three amide nitrogens such that each macrocyclic unit serves as a receptor for triflate anion, in a similar manner to that proposed for related cyclic peptide anion receptors (*8*).

While the metal centres are formally four–coordinated (Figure 6), the chloride anions are located in close proximity to the divalent palladium such that a contact (3.136(3) Å) exists between them creating a pseudo-square-based pyramidal arrangement, which is presumably stabilised by electrostatic attraction. This arrangement also allows four further favourable $C_{phenylene}H\cdots Cl$ and $C_{pyridyl}H\cdots Cl$ interactions to occur with H···Cl distances of 2.78–2.98 Å. Non-classical interactions of this type have been observed in a number of pyridyl and chloride-containing metal complexes (*22*).

The polymeric species formed upon the reaction of **1** and $[Pd(dppp)]^{2+}$ thus contains two distinct anion-binding pockets, which serve to bind both chloride and triflate in the solid state. Given the infinite polymeric arrangement of the complex this yields to the complementary binding of an infinite number of anions, such that one chloride anion

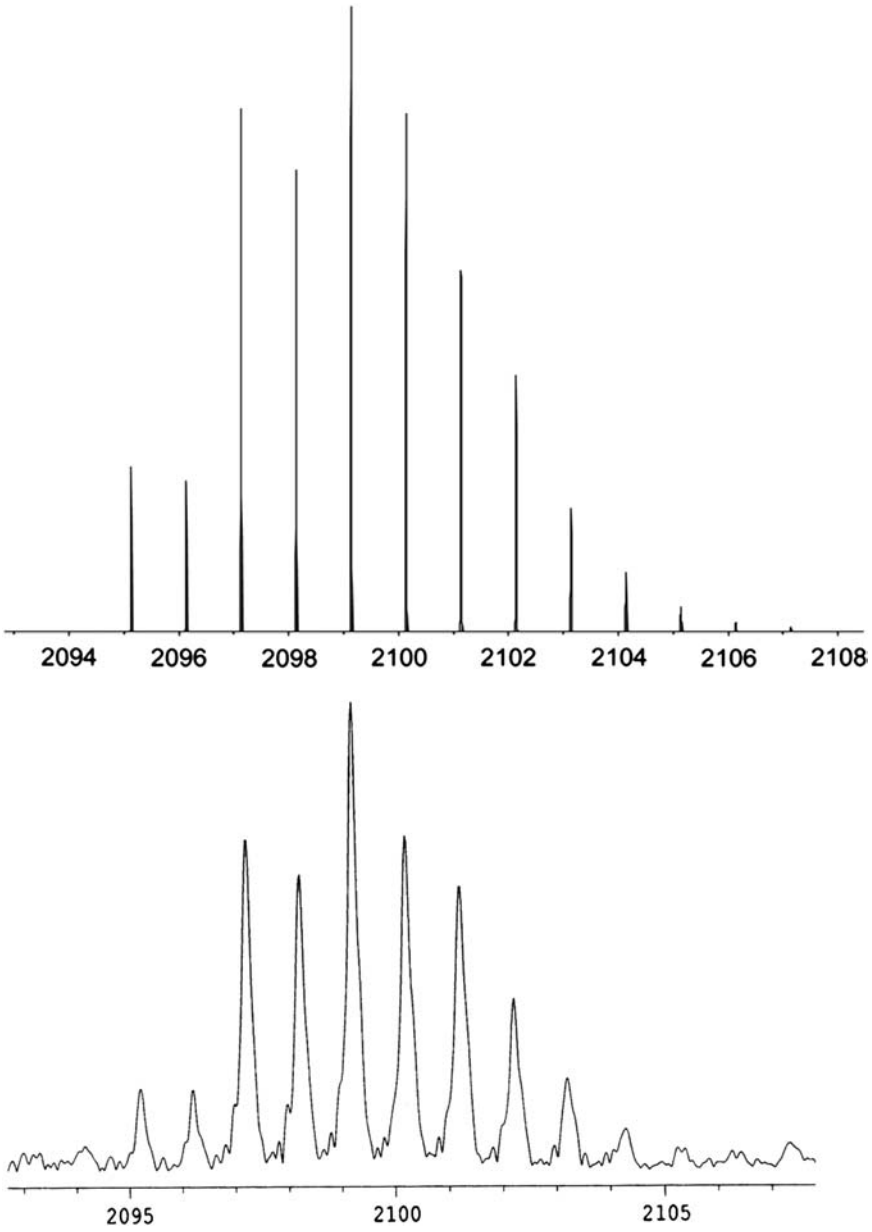

Figure 3. Calculated isotopic distribution for $[(C_{39}H_{39}N_9O_6S_3)_2Ag_3(NO_3)_2]^+$ (top); observed isotopic distribution for $[(C_{39}H_{39}N_9O_6S_3)_2Ag_3(NO_3)_2]^+$ (bottom).

and one triflate anion can be bound for each $[Pd(dppp)]^{2+}$ unit.

Conclusions

In summary, we have shown that the new cyclic peptide-derived tripodal ligand **1** can form either a molecular capsule in the presence of Ag(I) or a 1D infinite coordination polymer upon addition of Pd(II). Functionalisation of scaffold **2** with a range of ligands will provide new tripodal systems for the formation of further metallo-supramolecular structures with a variety of metal ions.

Experimental

General

Melting points were measured using a Stanford Research Systems Optimelt melting apparatus and are uncorrected. Optical rotations were performed using a PerkinElmer Model 341 polarimeter using the indicated spectroscopic grade solvents. ^1H and ^{13}C NMR spectra were recorded using either a Bruker Avance DPX 400/Bruker Avance DPX 300 spectrometer at a frequency of 300.13 MHz, or a Bruker Avance DPX 200 spectrometer and are reported as parts per million (ppm) downfield shift from tetramethylsilane using the residual solvent peak as reference. Low-resolution

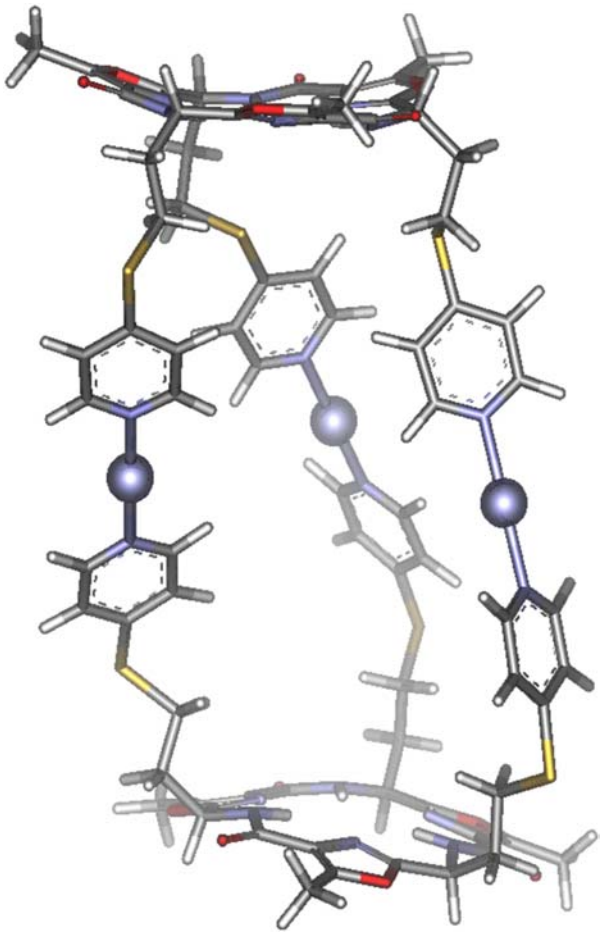

Figure 4. Molecular structure of the $(L_2Ag_3)^{3+}$ capsule modelled with SPARTAN 10 (AM1).

ESI mass spectra were recorded on a Thermo Finnigan LCQ Deca Ion Trap mass spectrometer. High resolution mass spectra (HRMS) were recorded on a Bruker BioApex Fourier Transform Ion Cyclotron Resonance mass spectrometer with an analytical ESI source, operating at 4.7 T. Preparative reversed-phase HPLC was performed on a Waters 600E multisolvent delivery system with a Waters U6K injector, Waters 490E programmable multiwavelength detector, Waters busSAT/IN module and Waters Empower 2 software.

Boc-Hse(Bn)-Thr-OMe (4)

A magnetically stirred solution of H-Thr-OMe·HCl (14.2 g, 83.7 mmol) in DMF (50 ml) was treated with NEt^iPr_2 (14.5 ml, 84 mmol) and maintained at 18°C for 0.5 h. The mixture was cooled to 0°C, and a solution of Boc-HSe(Bn)-OH (12.9 g, 41.7 mmol) in DMF (10 ml) and DPPA (13.5 ml, 62.5 mmol) was added. The resulting red solution was warmed to 18°C, and NEt^iPr_2 (29 ml, 166 mmol) was added via a dropping funnel. After 16 h, the reaction was quenched by the addition of water (30 mL), and all volatiles were removed by rotary evaporation. The resulting oil was treated with HCl (50 ml of a 1 M aq. solution) and extracted with EtOAc (4 × 200 ml). The combined organic fractions were dried ($MgSO_4$), and the solvent was removed under reduced pressure to give a yellow oil. Subjection of this material to flash chromatography (1:3 to 1:1, ethyl acetate–hexane) followed by concentration of the appropriate fractions ($R_f = 0.2$ in 1:1 ethyl acetate–hexane) gave the *dipeptide* ***4*** (11 g, 62%) as an oil that solidified to a white solid, m.p. 114°C, $[\alpha]_D + 3$ ($c = 1.8$ in $CHCl_3$) after prolonged storage (1 month). ^{1}H NMR ($CDCl_3$, 300 MHz) δ 7.39–7.27 (5H, complex m), 7.17 (1H, d, $J = 8.8$ Hz), 5.69 (1H, d, $J = 7.3$ Hz), 4.55 (1H, $J = 8.8$ and 2.7 Hz), 4.51 (2H, s), 4.38–4.23 (2H, m), 3.72 (3H, s), 3.63 (2H, m), 2.88 (1H, br s), 2.06 (2H, m), 1.43 (9H, s), 1.16 (3H, d, $J = 6.6$ Hz); ^{13}C NMR ($CDCl_3$, 75 MHz) δ 172.5 (C), 171.1 (C), 155.8 (C), 137.9 (C), 128.4 (CH), 127.8 (CH), 127.7 (CH), 80.0 (C), 73.3 (CH), 68.0 (C), 67.3 (CH_2), 57.4 (CH), 53.1 (CH), 52.4 (CH_3), 32.2 (CH_2), 28.3 (CH_3), 19.8 (CH_3); IR ν_{max} 3342, 2975, 2933, 2875, 1737, 1666, 1531, 914, 864 cm^{-1}; ESI-MS *m/z* 447 [$(M + Na)^+$, 100]; HRMS-ESI (*m/z*) calcd for $C_{21}H_{32}N_2O_7Na$ $(M + Na)^+$, 447.2210, found 447.2102.

Boc-Hse(Bn)-Thr(Oxz)-OMe (3)

A stirred solution of dipeptide **4** (5.01 g, 11.8 mmol) in anhydrous dichloromethane (160 mL) was cooled to −20°C under a nitrogen atmosphere. Deoxofluor (3.25 mL, 17.6 mmol) was added dropwise, and the mixture was stirred at −20°C for 1 h, then warmed to rt

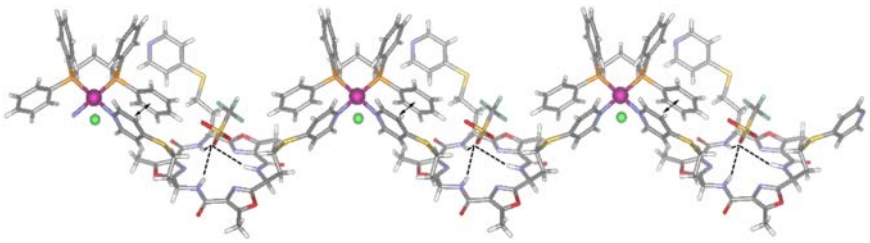

Figure 5. Part of the infinite 1D coordination polymer in the crystal structure of $\{[Pd(dppp)\mathbf{1}]\cdot OTf\cdot Cl\cdot 3MeOH\cdot 3Et_2O\}_n$. Dashed lines represent hydrogen bonds, and double-headed arrows represent π–π interactions. Regions of disorder removed for clarity.

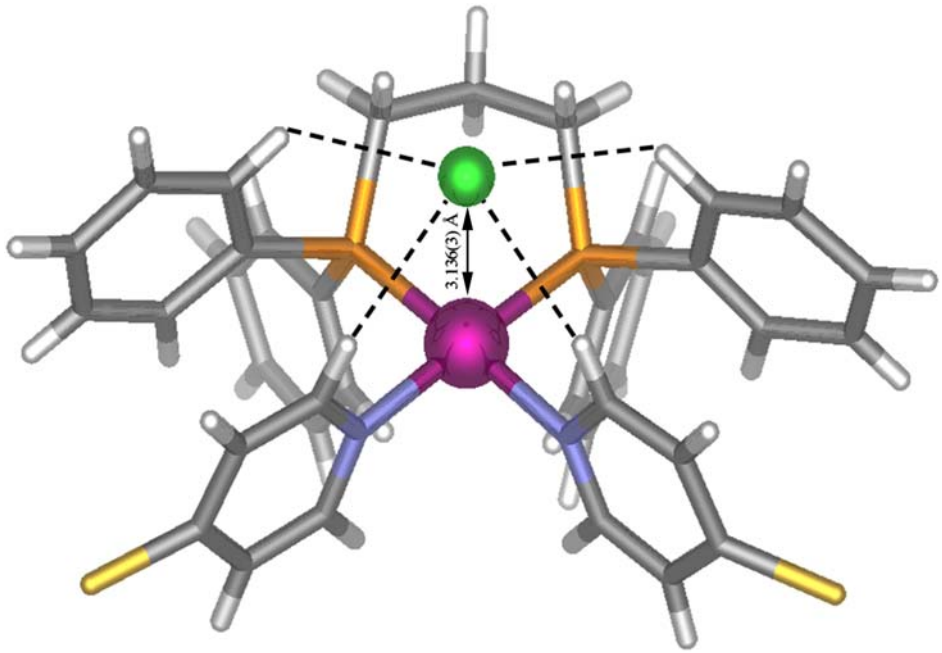

Figure 6. Schematic representation of part of the X-ray structure of $\{[Pd(dppp)\mathbf{1}]\cdot OTf\cdot Cl\cdot 3MeOH\cdot 3Et_2O\}_n$. Dashed lines indicate non-classical hydrogen bonds, and double-headed arrow indicates a short Pd–Cl contact.

and stirred for a further 6 h. The mixture was cooled to −20°C and quenched by the addition of saturated aqueous $NaHCO_3$ (70 mL) then allowed to warm slowly to rt with vigorous stirring. The resulting mixture was extracted with $CHCl_3$ (2 × 25 mL), and the combined organic phases were dried ($MgSO_4$) and concentrated under reduced pressure to give a yellow oil. The oil was dissolved in anhydrous dichloromethane (200 mL), and the solution was cooled to −20°C. Bromotrichloromethane (2.34 ml, 24.8 mmol) and DBU (3.69 mL, 24.75 mmol) were then added, and the mixture was allowed to warm slowly to rt and stirred for 6 h. The volume was reduced to 10 mL under reduced pressure, then a solution of saturated aqueous NH_4Cl (20 mL) was added. The resulting mixture was extracted with ethyl acetate (2 × 25 mL), then the combined organic phases were dried ($MgSO_4$) and concentrated under reduced pressure to give a brown oil. Subjection of this material to flash chromatography (2:3, ethyl acetate–hexane) followed by concentration of the appropriate fractions gave the *oxazole* ***3*** (2.39 g, 50%) as a colourless solid, m.p. 92–93°C; $[\alpha]_D$ −31 (*c* 2.1 in $CHCl_3$). ^{1}H NMR ($CDCl_3$, 300 MHz) δ 7.34–7.18 (5H, complex m), 5.58 (1H, m), 5.04 (1H, m), 4.43 (2H, m), 3.88 (3H, s), 3.54 (2H, t, $J = 5.8$ Hz), 2.53 (3H, s), 2.35 − 2.03 (2H, complex m), 1.42 (9H, s); ^{13}C NMR ($CDCl_3$, 75 MHz) δ 163.19 (C), 162.7 (C), 156.8 (C), 155.5 (C), 138.4 (C), 128.7 (CH), 128.0 (CH), 127.7 (C), 80.3 (C), 73.6 (CH_2), 66.8 (CH_2), 52.3 (CH_3), 47.6 (CH), 34.2 (CH_2), 28.7 (CH_3), 12.3 (CH_3; one signal obscured or overlapping); ESI-MS *m/z* 427 [$(M + Na)^+$, 100], 371 (43), 349 (14). HRMS-ESI (*m/z*) calcd for $C_{21}H_{28}N_2O_6Na$ $(M + Na)^+$, 427.1845, found 427.1830. Elemental analysis calculated for $C_{21}H_{28}N_2O_6$: C, 62.36; H, 6.98; N, 6.93. Found: C, 62.57; H, 6.90; N, 6.99%. Single crystals suitable for X-ray structure analysis were obtained by slow evaporation of an acetone solution.

Boc-Hse(Bn)-Thr(Oxz)-OPfp (7)

Methyl ester **3** (760 mg, 1.88 mmol) was dissolved in MeOH (12 ml), and H_2O (4 ml) was added. Solid NaOH (226 mg, 5.64 mmol) was added at rt, and the reaction mixture was stirred for 2 h, upon which all starting material had been consumed. MeOH was evaporated, and the resulting aqueous mixture was acidified to pH 5 with aqueous 1 M HCl solution (4 ml). The organic material was extracted with EtOAc (2 × 20 ml) and washed with brine solution (20 ml), dried ($MgSO_4$) and concentrated *in vacuo* leaving a sticky green foam. This was immediately dissolved in THF (19 ml), and DCC (465 mg, 2.26 mmol) followed by pentafluorophenol (415 mg, 2.26 mmol) was added at rt. The reaction mixture was stirred for 16 h after which time a white precipitate had formed. This was collected by Buchner filtration and washed with a little cold THF. The filtrate was concentrated *in vacuo* leaving an orange oil (1.39 g), which was purified by flash column chromatography (EtOAc:$CHCl_3$, 3:100) giving *pentafluorophenyl ester* **7** as a colourless oil (842 mg, 81% over two steps), $[\alpha]_D^{20}$ −27.6 (*c* = 1.0, $CHCl_3$); ^{1}H NMR (400 MHz, $CDCl_3$) δ 7.34–7.26 (5H, m), 5.65 (1H, d, $J = 7.3$ Hz),

5.08 (1H, app dd, $J = 7.3$, 5.7 Hz), 4.48 (1H, d, $J = 11.8$ Hz), 4.44 (1H, d, $J = 11.8$ Hz), 3.60 (2H, t, $J = 5.7$ Hz), 2.59 (3H, s), 2.28 (1H, dq, $J = 14.3$, 5.7 Hz), 2.18 (1H, dq, $J = 14.3$, 5.7 Hz), 1.44 (9H, s); ^{13}C NMR (100 MHz, $CDCl_3$) δ 163.2, 159.6, 157.9, 137.9, 128.4, 127.8, 127.7, 125.3, 80.3, 73.3, 66.5, 47.6, 33.7, 28.4, 12.4 (one signal obscured or overlapping); ESI-MS *m/z* 579 [$(M + Na)^+$, 100], 1134 [$(2M + Na)^+$, 18]; HRMS-ESI (*m/z*) found $[M + Na]^+$ 579.1531, $C_{26}H_{25}F_5N_2NaO_6$ requires $[M + Na]^+$ 579.1525.

H_2N-Hse(Bn)-Thr(Oxz)-OPfp·CF_3COOH (8)

TFA (12 ml) was added to a solution of Pfp ester **7** (842 mg, 1.51 mmol) in CH_2Cl_2 (4 ml) at rt. The reaction mixture was stirred for 2 h, and the solvents were removed leaving an orange oil. Toluene (2 × 10 ml) was added to azeotrope off remaining TFA, and the solvents were once again removed leaving the *TFA salt* **8** as an orange oil (861 mg, quantitative), $[\alpha]_D^{20} + 3.0$ ($c = 1.0$, MeOH); ^{1}H NMR (400 MHz, MeOD) δ 7.30–7.14 (5H, m), 4.79 (1H, t, $J = 6.5$ Hz), 4.47 (2H, s), 3.68 (2H, t, $J = 5.5$ Hz), 2.60 (3H, s), 2.44–2.35 (2H, app dt, $J = 6.5$, 5.5 Hz); ^{13}C NMR (100 MHz, MeOD) δ 162.5, 159.9, 158.7, 139.1, 129.4, 128.9, 128.8, 126.5, 118.6, 74.1, 66.6, 49.0, 32.8, 12.2; ESI-MS *m/z* 913 [$(2M + H)^+$, 100], 457 [$(M + H)^+$, 48], 935 [$(2M + Na)^+$, 39]; HRMS-ESI (*m/z*) found $[M + H]^+$ 457.1194, $C_{21}H_{18}F_5N_2O_4$ requires $[M + H]^+$ 457.1181.

Cyclo[Hse(Bn)-Thr(Oxz)]$_3$ (9) and Cyclo[Hse(Bn)-Thr(Oxz)]$_4$ (10) (Method 1)

The TFA salt **8** (861 mg, 1.51 mmol) was dissolved in DMF (30 ml) at rt, NEt^iPr_2 (0.77 ml, 4.53 mmol) was added, and the reaction mixture was stirred for 72 h, turning from pale orange to dark orange. DMF was removed on a rotary evaporator, and the resulting orange oil was dissolved in EtOAc (50 ml) and washed with 1 M HCl solution (2 × 50 ml). The aqueous fractions were back extracted with EtOAc (50 ml), and the combined organics were washed with half-saturated brine solution (50 ml), dried ($MgSO_4$) and concentrated *in vacuo* leaving an orange oil. This oil was subjected to a plug silica column (1:3 to 3:1, EtOAc:hexane) leaving an orange oil (330 mg). The cyclic products were separated from each other by preparative HPLC [Waters Sunfire C_{18} column, 19 mm, gradient elution 55–90% of MeCN:TFA (100:0.1)/H_2O:MeCN:TFA (95:5:0.1), flow rate = 7 ml/min: t_R (cyclic trimer **9**) = 46.9 min, t_R (cyclic tetramer **10**) = 51.7 min] leaving **9** (214 mg, 52%) and **10** (75 mg, 18%) as hygroscopic white solids after lyophilisation from ^{t}BuOH.

Cyclic trimer **9**: m.p. 46–47°C; $[\alpha]_D^{20}$ −4.8 ($c = 2.7$, $CHCl_3$); ^{1}H NMR (400 MHz, $CDCl_3$) δ 8.50 (3H, d, $J = 6.0$ Hz), 7.35–7.24 (15H, m), 5.26 (3H, q, $J = 6.0$ Hz), 4.46 (3H, d, $J = 11.7$ Hz), 4.35 (3H, d, $J = 11.7$ Hz), 3.70–3.60 (6H, m), 2.58 (9H, s), 2.44–2.39 (6H, m); ^{13}C NMR (100 MHz, $CDCl_3$) δ 161.2, 161.1, 153.9, 138.2, 128.4, 128.3, 127.6, 127.6, 73.0, 65.9, 46.1, 34.4, 11.6; IR ν_{max} 3381, 2927, 2860, 2359, 1676, 1639, 1585, 1519, 1452, 1436, 1392, 1369, 1265, 1200, 1146, 1111, 1078, 1041, 997, 902, 736, 698, 605; ESI-MS *m/z* 839 [$(M + Na)^+$, 50], 817 [$(M + H)^+$, 100], 455 (32), 399 (22), 233 (68). HRMS-ESI (*m/z*) calcd for $C_{45}H_{48}N_6O_9Na$ $(M + Na)^+$, 839.3380; found 839.3375.

Cyclic tetramer **10**: m.p. 61–63°C; $[\alpha]_D^{20}$ −131 ($c = 2.0$, $CHCl_3$); ^{1}H NMR (400 MHz, $CDCl_3$) δ 7.52 (4H, d, $J = 9.3$ Hz), 7.32–7.26 (20H, m), 5.53 (4H, m), 4.43 (8H, s), 3.51–3.42 (8H, m), 2.59 (12H, s), 2.17 (4H, m), 1.98 (4H, m); ^{13}C NMR (100 MHz, $CDCl_3$) δ 161.1, 160.9, 153.9, 138.2, 128.7, 128.4, 127.7, 127.7, 73.2, 66.6, 43.7, 33.4, 11.8. ESI-MS *m/z* 1090 [$(M + H)^+$, 100], 1112 [$(M + Na)^+$, 33]; HRMS-ESI (*m/z*) found $[M + H]^+$ 1089.4734, $C_{60}H_{65}N_8O_{12}$ requires $[M + H]^+$ 1089.4717.

H_2N-Hse(Bn)-Thr(Oxz)-OH·HCl (6)

A magnetically stirred solution of oxazole **4** (4.51 g, 11.16 mmol) in MeOH (40 mL) was cooled to 0°C, treated with NaOH (12.8 mL of a 2 M aq. solution) and allowed to warm to 18°C over 16 h. Subsequently, HCl (20 mL of a 1 M aq. solution) was added, and the mixture was extracted with $CHCl_3$-*iso*propyl alcohol (3 × 50 mL of a 3:1 v/v mixture). The combined organic fractions were dried ($MgSO_4$), and the solvent was removed under reduced pressure to give the free carboxylic acid as a yellow oil (4.229 g, 10.83 mmol). This was dissolved in 4 M HCl in dioxane (60 ml) at 0°C and was allowed to warm slowly to rt. Stirring was continued until TLC showed the consumption of all starting material (5 h). The mixture was concentrated under reduced pressure to yield the *HCl salt* **6** as a hygroscopic yellow oil (3.49 g, 96%). $[\alpha]_D^{20} = +13.7$ ($c = 0.526$, MeOH); ^{1}H NMR (200 MHz, MeOD) δ 7.31 (s, 5H, aromatic), 4.78 (s, 1 H, CH), 4.49 (s, 2 H, CH_2), 3.67–3.69 (m, 2 H, CH_2), 2.57 (s, 3 H, CH_3), 2.42 (m, 2 H, CH_2); ^{13}C NMR (75 MHz, MeOD) δ 165.72, 159.93, 159.64, 139.83, 130.24, 130.05, 129.77, 129.67, 74.93, 68.29, 33.54, 12.95. HRMS-ESI (*m/z*) calcd for $C_{15}H_{18}N_2O_4$ $[M + H]^+$ 291.13395, found 291.13435. Elemental analysis calculated for $C_{15}H_{19}ClN_2O_4.0.5\,H_2O$: C, 53.7; H, 5.7; N, 8.3. Found: C, 53.4; H, 6.1; N, 8.4%.

Cyclo[Hse(Bn)-Thr(Oxz)]$_3$ (9) (Method 2)

Oxazole **6** (3.30 g, 10.1 mmol) was dissolved in DMF (200 mL), treated sequentially with FDPP (8.45 g, 22.0 mmol) and NEt^iPr_2 (5.23 mL, 30.0 mmol), and the resulting mixture was stirred at 18°C for 5 days. Subsequently, excess DMF was removed under reduced pressure, and the residue was partitioned between HCl

(100 ml of a 1 M aq. solution) and $CHCl_3$-*iso*propyl alcohol (100 ml of a 3:1 v/v mixture). The separated aqueous fraction was extracted with $CHCl_3$-*iso*propyl alcohol (3 × 100 ml of a 3:1 v/v mixture), and the combined organic fractions were dried ($MgSO_4$) then the solvent was removed under reduced pressure to give a yellow residue. Subjection of this material of flash chromatography (1:3 to 1:1, ethyl acetate–hexane) followed by concentration of the relevant fractions ($R_f = 0.3$ in 1:1, ethyl acetate–hexane) gave the *cyclotrimer* **9** (1.15 g, 42%) as a yellow oil, data identical to that described above.

Cyclo[Hse-Thr(Oxz)]$_3$ (11)

Benzyl-protected trioxazole **9** (3.00 g, 3.68 mmol) was dissolved in a mixture of ethyl acetate (25 mL) and methanol (25 mL) in a glass pressure hydrogenation vessel under a stream of N_2. Palladium on charcoal (10%) was carefully added to the solution, and the mixture was agitated under H_2 for 12 h. The mixture was filtered through a Celite pad, and the Celite was washed with hot methanol. The organic filtrates were combined, and the solvent was removed under reduced pressure. The residue was purified by column chromatography (2% MeOH in CH_2Cl_2) to give the *triol* **11** as a colourless oil (2.00 g, 99%). $[\alpha]_D^{20} = -45$ ($c = 1.86$, MeOH); ^{1}H NMR (200 MHz, MeOD) δ 8.55 (3H, d, $J = 6.4$ Hz), 5.20 (3H, m), 3.61–3.69 (6H, m, CH_2), 2.63 (9H, s), 2.09–2.35 (6H, m); ^{13}C NMR (50 MHz, MeOD) δ 162.7, 162.4, 155.4, 129.3, 58.5, 46.9, 38.0, 11.6. HRMS-ESI (*m/z*) calcd for $C_{24}H_{30}N_6O_9$ $[M + Na]^+$ 569.1967, found 569.1965. Elemental analysis calculated for $C_{24}H_{30}N_6O_9.0.5H_2O$: C, 51.9; H, 5.6; N, 15.1. Found: C, 51.7; H, 5.5; N, 15.0%.

Tritosylate (12)

A solution of TsCl (3.14 g, 16.5 mmol) in acetonitrile (10 mL) was added slowly to a stirred solution of triol **11** (2.00 g, 3.66 mmol), Et_3N (2.78 g, 27.5 mmol) and Me_3-N·HCl (0.21 g, 2.20 mmol) in acetonitrile (10 mL) at 0°C, and the mixture was stirred for 3 h. Methanol (2 mL) was then added to decompose excess TsCl, and the mixture was stirred for a further 0.5 h. The solvent was removed under reduced pressure, and the residue was partitioned between chloroform (50 mL) and water (25 mL). The aqueous phase was extracted with chloroform (2 × 50 mL), then the combined organic fractions were washed with water and brine, dried ($MgSO_4$) and concentrated under reduced pressure. The residue was purified by column chromatography (0.5% MeOH in CH_2Cl_2) to give the desired *tritosylate* **12** as a colourless oil (3.50 g, 95%), $[\alpha]_D^{20} + 6.2$ ($c = 1.46$, $CHCl_3$); ^{1}H NMR (300 MHz, $CDCl_3$) δ 8.40 (3H, d, $J = 6.3$ Hz), 7.72 (6H, d, $J = 8.2$ Hz), 7.29 (6H, d, $J = 8.2$ Hz), 5.16 (3H, ddd, $J = 6.3$, 5.5, 5.5 Hz), 4.22 (6H, dd, $J = 6.2$, 6.2 Hz), 2.57 (9H, s), 2.40 (9H, s), 2.33–2.54 (6H, m); ^{13}C NMR (75 MHz, $CDCl_3$) δ 160.9, 159.7, 154.4, 144.8, 132.9, 129.8, 128.2, 127.8, 65.8, 45.3, 33.8, 21.5, 11.5. HRMS-ESI (*m/z*) calcd for $C_{45}H_{48}N_6O_{15}S_3$ $[M + H]^+$ 1009.2418, found 1009.2414.

Tribromide (2)

LiBr (0.255 g, 2.94 mmol) was added to a solution of **12** (0.247 g, 0.245 mmol) in anhydrous DMF (0.735 mL) at rt, and the resulting suspension was stirred at 55°C for 24 h. The mixture was diluted with water (5 mL) and extracted with $CHCl_3$-*iso*propyl alcohol (3 × 10 mL of a 3:1 v/v mixture). The combined organic phases were washed with water (5 mL) and brine (5 mL), dried ($MgSO_4$), and concentrated under reduced pressure. The residue was purified by column chromatography (0.5% MeOH in CH_2Cl_2) to afford the *tribromide* **2** as a white powder (0.152 g, 85%). Single crystals suitable for X-ray structure analysis were obtained by slow evaporation from a mixture of dichloromethane and methanol, m.p. 63–65°C; $[\alpha]_D^{20}$ −16.8 ($c = 2.66$, $CHCl_3$); ^{1}H NMR (200 MHz, $CDCl_3$) δ 8.36 (3H, d, $J = 6.4$ Hz), 5.24 (3H, ddd, $J = 6.4$, 6.1, 6.1), 3.41–3.61 (6H, m), 2.68 (9H, s, CH_3), 2.48–2.78 (6H, m); ^{13}C NMR (50 MHz, $CDCl_3$) δ 161.0, 159.9, 154.5, 128.4, 47.2, 38.1, 27.3, 11.7. HRMS-ESI (*m/z*) calcd for $C_{24}H_{27}Br_3N_6O_6$ $[M + Na]^+$ 756.9421, found 756.9422. Elemental analysis calculated for $C_{24}H_{27}Br_3N_6O_6$: C, 39.2; H, 3.7; N, 11.4. Found: C, 39.3; H, 3.7; N, 11.3%.

Tris-mercaptopyridine (1)

A suspension of **2** (70 mg g, 0.09 mmol) and Cs_2CO_3 (0.25 g, 0.77 mmol) in anhydrous acetonitrile (1 mL) was stirred for 1 h under a nitrogen atmosphere. A solution of 4-mercaptopyridine (0.43 g, 0.39 mmol) anhydrous acetonitrile (1 mL) was then added, and the solution was stirred at 0°C for a further 3 h. The solvent was removed under reduced pressure, and the residue was partitioned between chloroform (20 ml) and water (10 ml). The organic phase was washed with water (10 ml), dried ($MgSO_4$) and the solvent was removed under reduced pressure. The residue was purified by column chromatography ($CHCl_3$/CH_3-OH/CH_3CN; 25:1:1) to give the title compound as a white powder (62 mg, 84%), m.p. 58–59°C; $[\alpha]_D^{20} = -8.5$ ($c = 2.25$, $CHCl_3$); ^{1}H NMR (300 MHz, $CDCl_3$) 8.39 (9H, m), 7.09 (6H, d, $J = 9.3$), 5.28 (3H, m), 3.28–3.02 (6H, m), 2.67 (9 H, s), 2.58–2.47 (3H, m), 2.37–2.23 (3H, m); ^{13}C NMR (75 MHz, $CDCl_3$) δ 161.2 (C), 160.1 (C), 154.7 (C), 149.4 (CH), 148.3 (C), 128.8 (C), 120.9 (CH), 47.4 (CH), 34.0 (CH_2), 26.4 (CH_2), 11.7 (CH_3). HRMS-ESI (*m/z*) calcd for $C_{39}H_{39}N_9O_6S_3$ $[M + H]^+$ 826.2264, found 826.2279.

Elemental analysis calculated for $C_{39}H_{39}N_9O_6S_3.H_2O$: C, 55.5; H, 4.9; N, 14.9. Found: C, 55.8; H, 4.8; N, 14.5%.

Preparation of silver complex of 1

A solution of silver nitrate (27 mg, 0.016 mmol) in acetonitrile/methanol (4 mL, 1:1 v/v) was added to a solution of trispyridine **1** (9.0 mg, 0.011 mmol) in methanol/acetone (2 mL 1:1 v/v). The resulting precipitate was collected by filtration, washed with acetone and dried over P_2O_5 to give [($\mathbf{1}_2Ag_3(NO_3)_3$] as a colourless solid (11 mg, 95%). Elemental analysis calculated for $C_{78}H_{78}N_{21}O_{21}S_6Ag_3.2(C_3H_6O)$: C, 44.3; H, 4.0; N, 12.9; S, 8.5; Ag 14.2%. Found: C, 44.7; H, 3.9; N, 13.2; S, 8.3; Ag, 13.8%.

{[Pd(dppp)1]·OTf·Cl·3MeOH·3Et$_2$O}$_n$

A solution of Pd(dppp)OTf$_2$ (*21*) (7.4 mg, 9.0 mmol) in CD_3OD (0.35 mL) was added to a solution of **1** (5.0 mg, 6 mmol) in CD_3OD (0.35 mL) resulting in the immediate formation of a colourless precipitate. The CD_3OD was removed by blowing a stream of nitrogen across the sample, then $CDCl_3$ (0.7 mL) was added to dissolve the residue. Diethyl ether was slowly diffused into the sample resulting in the formation of a small number of colourless plate-like crystals. One of these was used directly in determination of the X-ray crystallographic structure of **{[Pd(dppp)1]·OTf·Cl·3MeOH·3Et$_2$O}$_n$**.

X-ray data

Data for **2** and **3** (see Supplementary Information available online for details of **3**) were collected with ω scans to approximately 56° 2θ using a Bruker SMART 1000 diffractometer employing graphite-monochromated Mo Kα radiation generated from a sealed tube (0.71073 Å) at 150(2) K. Data integration and reduction were undertaken with SAINT and XPREP (SMART, SAINT and XPREP Bruker Analytical X-ray Instruments Inc., Madison, WI, USA). Data for {[Pd(dppp)**1**]·OTf·Cl·3MeOH·3Et$_2$O}$_n$ were collected on a Bruker-Nonius APEX2-X8-FR591 diffractometer employing graphite-monochromated Mo–Kα radiation generated from a rotating anode (0.71073 Å) with ω and ψ scans to approximately 56° 2θ at 150(2) K (APEX v2.1, SAINT v.7 and XPREP v.6.14, Bruker AXS Inc., Madison, Wisconsin, USA, 2003). Subsequent computations were carried out using the WinGX-32 graphical user interface (*23*). Structures were solved by direct methods using SIR97 (*24*). Multi-scan empirical absorption corrections were applied to the data-set using the program SADABS (*25*). Data were refined and extended with SHELXL-97 (SHELX-97: Programs for Crystal Structure Analysis, University of Göttingen, 1997) (*26*). In general, non-hydrogen atoms with occupancies greater than 0.5 were refined anisotropically. Carbon-bound hydrogen atoms were included in idealised positions and refined using a riding model. Oxygen- and nitrogen-bound hydrogen atoms were first located in the difference Fourier map before refinement with bond length and angle restraints where required. Disorder was modelled using standard crystallographic methods including constraints and restraints where necessary. Crystallographic data are summarised below along with specific details regarding the refinement where required. CIFs (CCDC 870355–870357) have been deposited with the Cambridge Crystallographic Data Centre and can be obtained free of charge via http://www.ccdc.cam.ac.uk/conts/retrieving.html, or 12 Union Road, Cambridge CB2 1EZ, UK; fax: (+44) 1223-336-033; or e-mail: deposit@ccdc.cam.ac.uk.

Cyclic peptide 2

Formula $C_{25.125}H_{32.215}Br_3Cl_{0.50}N_6O_{7.50}$, *M* 795.75, monoclinic, space group $P2_1$(#4), *a* 12.9142(12), *b* 20.1964(19), *c* 12.9732(12) Å, β 106.964(2), *V* 3236.4(5) Å^3, D_c 1.633 g cm^{-3}, *Z* 4, crystal size 0.3 × 0.1 × 0.05 mm, colour colourless, habit needle, temperature 150(2) K, λ(Mo Kα) 0.71073 Å, μ(MoKα) 3.833 mm^{-1}, T(SADABS)$_{min,max}$ 0.595956, 1.000000, $2\theta_{max}$ 56.62, *hkl* range −16 16, −26 25, −16 16, *N* 31,950, N_{ind} 14,996(R_{merge} 0.0524), N_{obs} 7438(I > 2σ(I)), N_{var} 861, residuals* *R*1(*F*) 0.0832, *wR*2(F^2) 0.2606, GoF(all) 0.973, $\Delta\rho_{min,max}$ −0.766, 0.915 e$^-$ Å^{-3}.

*$R1 = \Sigma||F_o|-|F_c||/\Sigma|F_o|$ for $F_o > 2\sigma(F_o)$; $wR2 = (\Sigma w(F_o^2-F_c^2)^2/\Sigma(wF_c^2)^2)^{1/2}$ all reflections $w = 1/[\sigma^2(F_o^2) + (0.1535P)^2 + 0.0000P]$ where $P = (F_o^2 + 2F_c^2)/3$.

Specific refinement details

Each of the bromoethyl side chains except the Br(6) containing arm is disordered over a number of positions and a number of constraints and restraints (including the use of some constrained isotropic displacement parameters on low occupancy bromine atoms) were required to facilitate realistic modelling. The solvent is also significantly disordered; the dichloromethane was modelled over two 0.25 occupancy positions (each with identical isotropic displacement parameters). The methanol was modelled over four positions with a total occupancy of 2.25, and the water was modelled over two positions of 0.5 and 0.25. The oxygen-bound hydrogen atoms could not be located in the difference Fourier map and were not modelled.

{[Pd(dppp)1]·OTf·Cl·3MeOH·3Et$_2$O}$_n$

Formula $C_{82}H_{107}ClF_3N_9O_{15}P_2PdS_4$, *M* 1847.80, trigonal, space group $P3_121$(#152), *a* 19.3608(3), *b* 19.3608(3), *c* 36.6284(13) Å, γ 120.00°, *V* 11,890.4(5) Å^3, D_c 1.548 g

cm^{-3}, *Z* 6, crystal size 0.3 × 0.3 × 0.01 mm, colour colourless, habit plate, temperature 150(2) K, λ(Mo Kα) 0.71073 Å, μ(Mo Kα) 0.495 mm^{-1}, $T(SADABS)_{min,max}$ 0.710509, 1.000000, $2\theta_{max}$ 56.50, *hkl* range −25 25, −24 24, −41 48, *N* 110,846, N_{ind} 19,480(R_{merge} 0.0704), N_{obs} 12,009(I > 2σ(I)), N_{var} 736, residuals* *R*1(*F*) 0.0821, *wR*2(F^2) 0.2431, GoF(all) 0.982, $\Delta\rho_{min,max}$ −1.166, 1.606 $e^- Å^{-3}$.

*$R1 = \Sigma||F_o|-|F_c||/\Sigma|F_o|$ for $F_o > 2\sigma(F_o)$; $wR2 = (\Sigma w(F_o^2-F_c^2)^2/\Sigma(wF_c^2)^2)^{1/2}$ all reflections $w = 1/[\sigma^2(F_o^2) + (0.1628P)^2 + 0.0000P]$ where $P = (F_o^2 + 2F_c^2)/3$.

Specific refinement details

The S(3) arm of the ligand is disordered over two positions with occupancies of 0.7 and 0.3, which were modelled with equal anisotropic displacement parameters and a number of bond length and angle restraints. Both the S(1) containing arm and the triflate anion display a significant amount of thermal motion and/or unresolved disorder. Accordingly, both bond length and angle restraints along with thermal parameter restraints were required. In addition to these problems, there is a significant amount of unresolved electron density present in the lattice. Despite numerous attempts at modelling this disorder including the use of rigid bodies, no satisfactory model could be found, and accordingly, the SQUEEZE (*27*) function of PLATON (*28*) was employed to remove the contributions of this unresolved electron density from the model.

Acknowledgements

We thank the Australian Research Council for funding (DP0555883) and Dr Nicholas Proschogo (The University of Sydney) for assistance with mass spectral data.

References

(1) Thomas, J.A. *Dalton Trans*. **2011**, 40, 12005–12016. Hristova, Y.R.; Smulders, M.M.J.; Clegg, J.K.; Breiner, B.; Nitschke, J.R. *Chem. Sci.* **2011**, *2*, 638–641. Meng, W.; Breiner, B.; Rissanen, K.; Thoburn, J.D.; Clegg, J.K.; Nitschke, J.R. *Angew. Chem. Int. Ed.* **2011**, *50*, 3479–3483. Stephenson, A.; Argent, S.P.; Tidmarsh, I.S.; Ward, M.D. *J. Am. Chem. Soc.* **2011**, *133*, 858–870. Riddell, I.A.; Smulders, M.M.J.; Clegg, J.K.; Nitschke, J.R. *Chem. Commun.* **2011**, *47*, 457–459. Breiner, B.; Clegg, J.K.; Nitschke, J.R. *Chem. Sci.* **2011**, *2*, 51–56. Sun, Q.-F.; Iwasa, J.; Ogawa, D.; Ishido, Y.; Sato, S.; Ozeki, T.; Sei, Y.; Yamaguchi, K.; Fujita, M. *Science* **2010**, *328*, 1144–1147. Mal, P.; Breiner, B.; Rissanen, K.; Nitschke, J.R. *Science* **2009**, *324*, 1697–1699. Ward, M.D. *Chem. Commun.* **2009**, 4487–4499. Pluth, M.D.; Bergman, R.G.; Raymond, K.N. *Acc. Chem. Res.* **2009**, *42*, 1650–1659. Northrop, B.H.; Zheng, Y.-R.; Chi, K.-W.; Stang, P.J. *Acc. Chem. Res.* **2009**, *42*, 1554–1563. Yoshizawa, M.; Klosterman, J.K.; Fujita, M. *Angew. Chem. Int. Ed.* **2009**, *48*, 3418–3438. Saalfrank, R.W.; Maid, H.; Scheurer, A. *Angew. Chem. Int. Ed.* **2008**, *47*, 8794–8824. Tranchemontagne, D.J.; Ni, Z.; O'Keeffe, M.; Yaghi, O.M. *Angew. Chem. Int. Ed.* **2008**, *47*, 5136–5147. Tidmarsh, I.S.; Faust, T.B.; Adams, H.; Harding, L.P.; Russo, L.; Clegg, W.; Ward, M.D. *J. Am. Chem. Soc.* **2008**, *130*, 15167–15175. Dalgarno, S.J.; Power, N.P.; Atwood, J.L. *Coord. Chem. Rev.* **2008**, *252*, 825–841. Fujita, M.; Tominaga, M.; Hori, A.; Therrien, B. *Acc. Chem. Res.* **2005**, *38*, 369–378. Fiedler, D.; Leung, D.H.; Bergman, R.G.; Raymond, K.N. *Acc. Chem. Res.* **2005**, *38*, 349–358.

(2) Gardner, J.S.; Harrison, R.G.; Lamb, J.D.; Dearden, D.V. *New J. Chem.* **2006**, *30*, 1276–1282. McKinlay, R.M.; Cave, G.W.V.; Atwood, J.L. *Proc. Nat. Acad. Sci. USA*. **2005**, *102*, 5944–5948. Zuccaccia, D.; Pirondini, L.; Pinalli, R.; Dalcanale, E.; Macchioni, A. *J. Am. Chem. Soc.* **2005**, *127*, 7025–7032. Harrison, R.G.; Burrows, J.L.; Hansen, L.D. *Chem. Eur. J.* **2005**, *11*, 5881–5888. Pirondini, L.; Bertolini, F.; Cantadori, B.; Ugozzoli, F.; Massera, C.; Dalcanale, E. *Proc. Nat. Acad. Sci. USA*. **2002**, *99*, 4911–4915.

(3) Yamanaka, M.; Toyoda, N.; Kobayashi, K. *J. Am. Chem. Soc*. **2009**, *131*, 9880–9881. Haino, T.; Kobayashi, M.; Fukazawa, Y. *Chem. Eur. J*. **2006**, *12*, 3310–3319. Yamanaka, M.; Yamada, Y.; Sei, Y.; Yamaguchi, K.; Kobayashi, K. *J. Am. Chem. Soc*. **2006**, *128*, 1531–1539. Kobayashi, K.; Yamada, Y.; Yamanaka, M.; Sei, Y.; Yamaguchi, K. *J. Am. Chem. Soc*., **2004**, *126*, 13896–13897.

(4) Ronson, T.K.; Fisher, J.; Harding, L.P.; Hardie, M.J. *Angew. Chem. Int. Ed*. **2007**, *46*, 9086–9088. Sumby, C.J.; Gordon, K.C.; Walsh, T.J.; Hardie, M.J. *Chem. Eur. J.* **2008**, *14*, 4415–4425. Ronson, T.K.; Carruthers, C.; Fisher, J.; Brotin, T.; Harding, L.P.; Rizkallah, P.J.; Hardie, M.J. *Inorg. Chem.* **2010**, *49*, 675–685. Carruthers, C.; Ronson, T.K.; Sumby, C.J.; Westcott, A.; Harding, L.P.; Prior, T.J.; Rizkallah, P.; Hardie, M.J. *Chem. Eur. J.* **2008**, *14*, 10286–10296. Sumby, C.J.; Fisher, J.; Prior, T.J.; Hardie, M.J. *Chem. Eur. J.* **2006**, *12*, 2945–2959. Sumby, C.J.; Hardie, M.J. *Angew. Chem. Int. Ed.* **2005**, *44*, 6395–6399.

(5) Batten, S.R.; Neville, S.M.; Turner, D.R. *Coordination Polymers: Design, Analysis and Application*, RSC Publishing, Cambridge, 2009. Noro, S.; Kitagawa, S.-i.; Akutagawa, T.; Nakamura, T. *Prog. Polym. Sci*., **2009**, *34*, 240–279. Kitigawa, S.; Kitaura, R.; Noro, S.-i. *Angew. Chem. Int. Ed*., **2004**, *43*, 2334–2375.

(6) Wipf, P.; in *Alkaloids: Chemical and Biological Perspectives,* ed. Pelletier, S.W.; Elsevier, Amsterdam, 1998, vol 12, pp. 187–228. Wipf, P.; *Chem. Rev.* **1995**, *95*, 2115–2134. Mink, D.; Mecozzi, S.; Rebek, Jr., J. *Tetrahedron* **1998**, *39*, 5709–5712. Lucke, A.J.; Tyndall, J.D.A.; Singh, Y.; Fairlie, D.P.J. *Mol. Graph. Model.* **2003**, *21*, 341–355. Singh, Y.; Stoermer, M.J.; Lucke, A.J.; Guthrie, T.; Fairlie, D.P. *J. Am. Chem. Soc.* **2005**, *127*, 6563–6572. Jolliffe, K.A. *Supramol. Chem.* **2005**, *17*, 81–86. Pintér, A.; Haberhauer, G. *Synlett* **2009**, 3082–3089.

(7) McDonough, M.J.; Reynolds, A.J.; Lee, W.Y.G.; Jolliffe, K.A. *Chem. Commun*. **2006**, 2971–2973. Schnopp, M.; Ernst, S.; Haberhauer, G. *Eur. J. Org. Chem.* **2009**, 213–222. Young, P.G.; Jolliffe, K.A. *Org. Biomol. Chem*. **2012**, *10*, 2664–2672.

(8) Young, P.G.; Clegg, J.K.; Bhadbhade, M.; Jolliffe, K.A. *Chem. Commun.* **2011**, *47*, 463–465. Young, P.G.; Clegg, J.K.; Jolliffe, K.A. *Supramol. Chem*. **2011**, *24*, 77–87.

(9) Bertram, A.; Pattenden, G. *Nat. Prod. Rep*. **2007**, *24*, 18–30. Wipf, P.; Wang, C. *Org. Lett.* **2006**, *8*, 2381–2384. Bernhardt, P.V.; Comba, P.; Fairlie, D.P.; Gahan, L.R.; Hanson, G.R.; Lötzbeyer, L. *Chem. Eur. J*. **2002**, *8*, 1527–1536.
(10) Haberhauer, G.; Oeser, T.; Rominger, F. *Chem. Commun.* **2004**, 2044–2945.
(11) Singh, Y.; Stoermer, M.J.; Lucke, A.J.; Glenn, M.P.; Fairlie, D.P. *Org. Lett.* **2002**, *4*, 3367–3370.
(12) Jantos, K.; Rodriguez, R.; Ladame, S.; Shirude, P.S.; Balasubranian, S. *J. Am. Chem. Soc.* **2006**, *128*, 13662. Minhas, G.S.; Pilch, D.S.; Kerrigan, J.E.; LaVoie, E.J.; Rice, J.E. *Bioorg. Med. Chem. Lett*. **2006**, *16*, 3891.
(13) Haberhauer, G.; Oeser, T.; Romiger, F. *Chem. Commun*. **2005**, 2799–2801. Pintér, A.; Haberhauer, G. *Eur. J. Org. Chem*. **2008**, 2375–2387. Pintér, A.; Haberhauer, G. *Chem. Eur. J*. **2008**, *14*, 11061–11068. Zeigler, E.; Haberhauer, G. *Eur. J. Org. Chem*. **2009**, 3432–3438.
(14) Singh, Y.; Sokolenko, N.; Kelso, M.J.; Gahan, L.R.; Abbenante, G.; Fairlie, D.P. *J. Am. Chem. Soc.* **2001**, *123*, 333–334. Pattenden, G.; Thompson, T. *Chem. Commun.* **2001**, 717–718. Pattenden, G.; Thompson, T. *Tetrahedron Lett.* **2002**, *43*, 2459–2461. Haberhauer, G.; Oeser, T.; Romiger, F. *Chem. Eur. J*. **2005**, *11*, 6718–6726.
(15) Yue, N.L.S.; Jennings, M.C.; Puddephatt, R.J. *Inorg. Chem*. **2005**, *44*, 1125–1131. Yue, N.L.S.; Eisler, D.J.; Jennings, M.C.; Puddephatt, R.J. *Inorg. Chem*. **2004**, *43*, 7671–7681. Fujita, M.; Ogura, K. *Coord. Chem. Rev.* **1996**, *148*, 249–264. Kim, J.; Ryu, D.; Sei, Y.; Yamaguchi, K.; Ahn, K.H. *Chem. Commun.* **2006**, 1136–1138. Maurizot, V.; Yoashizawa, M.; Kawano, M.; Fujita, M. *Dalton Trans*. **2006**, 2750–2756. Hof, F.; Craig, S.L.; Nuckolls, C.; Rebek, Jr., J. *Angew. Chem. Int. Ed.* **2002**, *41*, 1488–1508. Kiehne, U.; Weilandt, T.; Lutzen, A. *Eur. J. Org. Chem.* **2008**, 2056–2064.
(16) Bray, D.J.; Liao, L.-L.; Antonioli, B.; Gloe, K.; Lindoy, L.F.; McMurtrie, J.C.; Wei, G.; Zhang, X.-Y. *Dalton Trans.* **2005**, *12*, 2082–2083.
(17) Butler, S.J.; Jolliffe, K.A. *Org. Biomol. Chem*. **2011**, *9*, 3471–3483. Butler, S.J.; Jolliffe, K.A.; Lee, W.Y.G.; McDonough, M.M.; Reynolds, A.J. *Tetrahedron* **2011**, *67*, 1019–1029. Bertram, A.; Blake, A.J.; Gonzaléz-López de Turiso, F.; Hannam, J.S.; Jolliffe, K.A.; Pattenden G.; Skae, M. *Tetrahedron* **2003**, *59*, 6979–6990.
(18) Black, R.J.G.; Dungan, V.J.; Li, R.Y.T.; Young, P.G.; Jolliffe, K.A. *Synlett* **2010**, 551–554. Bertram, A.; Hannam, J.S.; Jolliffe, K.A.; Gonzaléz-López de Turiso, F.; Pattenden, G. *Synlett* **1999**, 1723–1726. Jayaprakash, S.; Pattenden, G.; Viljoen, M.S.; Wilson, C. *Tetrahedron* **2003**, *59*, 6637–6646. Dudin, L.; Pattenden, G.; Viljoen, M.S.; Wilson, C. *Tetrahedron* **2005**, *61*, 1257–1267. Wipf, P.; Miller, C.P.; Grant, C.M. *Tetrahedron* **2000**, *56*, 9143. Haberhauer, G.; Somogyi, L.; Rebek, Jr., J. *Tetrahedron Lett.* **2000**, *41*, 5013–5016. Somogyi, L.; Haberhauer, G.; Rebek, Jr., J. *Tetrahedron* **2001**, *57*, 1699–1708. Haberhauer, G.; Romiger, F. *Tetrahedron Lett*. **2002**, *43*, 6335–6338. Haberhauer, G.; Romiger, F. *Eur. J. Org. Chem*. **2003**, 3209–3218. Haberhauer, G.; Oeser, T.; Romiger, F. *Chem. Commun*. **2004**, 2044–2046. Haberhauer, G. *Synlett* **2004**, 1003–1006. Boss, C.; Rasmussen, P.H.; Wartini, A.R.; Waldvogel, S.R. *Tetrahedron Lett*. **2000**, *41*, 6327–6331. Mink, D.; Mecozzi, S.; Rebek, Jr., J. *Tetrahedron Lett.* **1998**, *39*, 5709–5712.
(19) Phillips, A.J.; Uto, Y.; Wipf, P.; Reno, M.J.; Williams, D.R. *Org. Lett.* **2000**, *2*, 1165–1168.
(20) Flack, H.D. *Acta Cryst.* **1983**, *A39*, 876–881.
(21) Stang, P.J.; Cao, D.H.; Saito, S.; Arif, A.M. *J. Am. Chem. Soc.* **1995**, *117*, 6273–6283.
(22) Antonioli, B.; Bray, D.J.; Clegg, J.K.; Gloe, K.; Gloe, K.; Jaeger, A.; Jolliffe, K.A.; Kataeva, O.; Lindoy, L.F.; Steel, P.J.; Sumby, C.J.; Wenzel, M. *Polyhedron* **2008**, *27*, 2889–2898. Antonioli, B.; Buechner, B.; Clegg, J.K.; Gloe, K.; Gloe, K.; Goetzke, L.; Heine, A.; Jaeger, A.; Jolliffe, K.A.; Kataeva, O.; Kataev, V.; Klingeler, R.; Krause, T.; Lindoy, L.F.; Popa, A.; Seichter, W.; Wenzel, M. *Dalton Trans.* **2009**, 4795–4805. Kim, M.; Mora, C.; Lee, Y.H.; Clegg, J.K.; Lindoy, L.F.; Min, K.S.; Thuery, P.; Kim, Y. *Inorg. Chem. Commun.* **2010**, *13*, 1148–1151.
(23) Farrugia, L.J. *J. Appl. Cryst.* **1999**, *32*, 837–838.
(24) Altomare, A.; Burla, M.C.; Camalli, M.; Cascarano, G.L.; Giocavazzo, C.; Gaugliardi, A.; Moliterni, G.C.; Polidori, G.; Spagna, S. *J. Appl. Cryst.* **1999**, *32*, 115–119.
(25) SADABS: Empirical Absorption and Correction Software, University of Göttingen, **1996–2008**.
(26) Sheldrick, G.M. *Acta Cryst. A* **2008**, *64*, 112.
(27) van der Sluis, P.; Spek, A.L. *Acta Crystallogr. Sect. A* **1990**, *46*, 194–201.
(28) PLATON: A Multipurpose Crystallographic Tool, Utrecht University, **2008**.